



1 **Spatially explicit global gross domestic product (GDP) data**  
2 **set consistent with the Shared Socioeconomic Pathways**

3

4 Tingting Wang<sup>1</sup>, Fubao Sun<sup>1,2,3,4\*</sup>

5

6 1. Key Laboratory of Water Cycle and Related Land Surface Processes, Institute of  
7 Geographic Sciences and Natural Resources Research, Chinese Academy of Sciences,  
8 Beijing, China

9 2. State Key Laboratory of Desert and Oasis Ecology, Xinjiang Institute of Ecology and  
10 Geography, Chinese Academy of Sciences, Urumqi 830011, China

11 3. Akesu National Station of Observation and Research for Oasis Agro-ecosystem,  
12 Akesu, China

13 4. College of Resources and Environment, University of Chinese Academy of Sciences,  
14 Beijing, China

15

16

17 **Corresponding Author:** Fubao Sun (Sunfb@igsnr.ac.cn), from Key Laboratory of  
18 Water Cycle and Related Land Surface Processes, Institute of Geographic Sciences and  
19 Natural Resources Research, Chinese Academy of Sciences

20

21

22



## 23 **Abstract**

24       The increasing demand of ScenarioMIP is calling for GDP projections of high  
25 resolution for the future Shared Socioeconomic Pathways (SSPs) in both  
26 socioeconomic development and in climate change of adaption and mitigation research.  
27 While to date the global GDP projections for five SSPs are mainly provided at national  
28 scales, and the gridded data set are very limited. Meanwhile, the historical GDP can be  
29 disaggregated using nighttime light (NTL) images but the results are not open accessed,  
30 making it cumbersome in climate change impact and socioeconomic risk assessments  
31 across research disciplines. To this end, we produce a set of spatially explicit global  
32 Gross Domestic Product (GDP) that presents substantial long-term changes of  
33 economic activities for both historical period (2005 as representative) and for future  
34 projections under all five SSPs with a spatial resolution of 30 arc-seconds. Chinese  
35 population in SSP database were first replaced by the projections under the two-children  
36 policy implemented since 2016 and then used to spatialize global GDP using NTL  
37 images and gridded population together as fixed base map, which outperformed at  
38 subnational scales. The GDP data are consistent with projections from the SSPs and are  
39 freely available at <http://doi.org/10.5281/zenodo.4350027> (Wang and Sun, 2020). We  
40 also provide another set of spatially explicit GDP using the global LandScan population  
41 as fixed base map, which is recommended at county or even smaller scales where NTL  
42 images are limited. Our results highlight the necessity and availability of using gridded  
43 GDP projections with high resolution for scenario-based climate change research and  
44 socioeconomic development that are consistent with all five SSPs.

45

46



## 47 **1 Introduction**

48       The development of socioeconomic projection scenarios plays a key role in the  
49 assessment of climate change impact and socioeconomic risks for the coming decades  
50 (O'Neill et al., 2014; Wilbanks and Ebi, 2014). The Shared Socioeconomic Pathways  
51 (SSPs), which qualitative and quantitative describe broad patterns of possible global  
52 socioeconomic development with assumptions about climate change and policy  
53 responses under different challenges to mitigation and adaptation (O'Neill et al., 2014),  
54 are one of the core contents in the Intergovernmental Panel on Climate Change (IPCC)  
55 scientific assessment reports (IPCC, 2014) and in the current literature (O'Neill et al.,  
56 2016; Wilbanks and Ebi, 2014). The climate projection scenarios in Scenario Model  
57 Intercomparison Project (ScenarioMIP) are formed based on different SSPs  
58 corresponding to specific representative concentration pathways (RCPs) within Phase  
59 6 of the Coupled Model Intercomparison Project (CMIP6) (O'Neill et al., 2016).  
60 Scenarios of future socioeconomic impact on the global environment are built upon  
61 projections of economic output and strongly require socioeconomic data support of  
62 higher spatial resolution for the coming decades (B. Merz et al., 2010; O'Neill et al.,  
63 2016; Wilbanks and Ebi, 2014).

64       The Gross Domestic Product (GDP) is a standard indicator to assess and compare  
65 economic development within and across countries (Kummu et al., 2018; Nordhaus,  
66 2011; Tobias, 2018), and is usually collected at national scale (Tobias, 2018). However,  
67 the collection of official GDP data at a finer resolution (e.g., at state, city or county  
68 levels) is problematic, especially in many developing countries (Kummu et al., 2018;  
69 Nordhaus, 2011). It is crucial to spatialize GDP data into a fine-scale so that it can be  
70 easily integrated with data from other disciplines (Chen et al., 2020; Kummu et al.,  
71 2018; O'Neill et al., 2016). A growing number of openly available historical GDP data  
72 sets are provided with the development of satellite-derived nighttime light (NTL)  
73 images and gridded population to support current research at various spatial scales in a  
74 more convenient way (Bennett and Smith, 2017; Doll et al., 2006; Ghosh et al., 2010;  
75 Nordhaus, 2011; Zhao et al., 2017). The Defense Meteorological Satellite Program's



76 Operational Linescan System (DMSP-OLS) NTL imagery has been successfully used  
77 in GDP redistribution for 1992-2013. However, the disaggregated GDP depends highly  
78 on the DN values where a certain number of saturated pixels exist in DMSP-OLS NTL  
79 images, resulting in underestimations in urban centers and overestimations in rural  
80 regions (Zhu et al., 2017) but can be revised when incorporating with other ancillary  
81 data like gridded population (Zhao et al., 2017). The global Soumi National Polar-  
82 Orbiting Partnership Visible Infrared Imaging Radiometer Suite (NPP-VIIRS) NTL  
83 imagery made up this saturation problem and advanced its calibration, providing a more  
84 accurate approach in GDP downscaling since 2012 (Bennett and Smith, 2017). More  
85 research on reduction in exposure and vulnerability and increase in resilience to climate  
86 extremes can benefit from a spatially explicit GDP data set with increasing precision of  
87 NTL image products and population count at grid level (Chen et al., 2017; Chen et al.,  
88 2020; Wang et al., 2019; Wilbanks and Ebi, 2014).

89 However, the widely used GDP projections in the SSP database were provided only  
90 at national and super-national scales from several global institutes, which have depicted  
91 a wide range of uncertainty within different organizations (Riahi et al., 2017) and  
92 limited the usage of integration with data from other disciplines. Moreover, the spatially  
93 explicit global gridded GDP projections for all five SSPs are very limited, and  
94 Murakami and Yamagata (2019) have downscaled the global population and GDP for  
95 SSP1-3 only. Worse still, most socioeconomic development indicators for like the total  
96 factor productivity, capital stock, and labor input etc., are either short of data sources or  
97 provided mainly at national scale without proper conditions to make spatially explicit  
98 GDP predictions for future scenarios. The increasing vulnerability, exposure and  
99 resilience of socioeconomic activities to climate extremes are driving a need to move  
100 beyond administrative unit-based analyses to enable flexible integration with datasets  
101 of spatially explicit population and economic activities of long-term SSPs (Chen et al.,  
102 2017; Jones et al., 2015; Su et al., 2018; Winsemius et al., 2016).

103 Government policy change has a strong effect on GDP and should be taken into  
104 account for credible and quantitative information on demographic changes and  
105 socioeconomic development (Huang et al., 2019). The one-child for each couple policy



106 implemented in China since the late 1970s has been replaced by the two-children policy  
107 since 2016, and would no doubt have a substantial effect on the demographic  
108 composition, the total population and GDP projections in China in the long run.  
109 However, this policy was implemented after the release of population and GDP  
110 projections in the SSP database. Jiang et al., (2017; 2018) have updated Chinese  
111 population and GDP projections at provincial level that qualitatively consistent with  
112 five SSP narratives, showing that the implementation of two-children policy can  
113 mitigate the labor shortages and aging problems in China to a certain extent, and are  
114 expected to a 38.1 – 43.9% increase in GDP in the late 21st century (Huang et al., 2019).  
115 It would be beneficial to update SSP database of long-term demographic and economic  
116 projections in China with consideration of this two-children policy for future GDP  
117 downscaling for spatial analyses.

118 To date, there is no global gridded GDP for all five SSPs provided, and historical  
119 dataset are mainly based on national GDP from the World Bank and then redistributed  
120 using NTL images with other auxiliary information but are not open accessed. There is  
121 a growing demand for spatially explicit GDP that can represent different patterns of  
122 development and are consistent with all five SSPs to match the ScenarioMIP research.  
123 The objective of this study is to present a set of spatially explicit global GDP that  
124 presents substantial long-term changes of GDP for both historical period (2005 as  
125 representative) and for future projections under all five SSPs by incorporating various  
126 data sources and methods. In the following were the inputs, assumptions,  
127 methodologies, and results that we use to spatialize GDP data into a fine-scale,  
128 providing an alternative choice for scenario-based climate change research and  
129 socioeconomic development pathways.

130

## 131 **2 Data**

### 132 **2.1 Historical Population**



133 The distribution of population count (density) is a core indicator in measuring,  
134 mapping and assessing the exposure, vulnerability, and resilience of socioeconomic  
135 activities to climate extremes (Leyk et al., 2019). Several well-known global population  
136 data sets, namely the Gridded Population of the World (GPW), the Global Rural Urban  
137 Mapping Project (GRUMP), the WorldPop, and the LandScan Global Population  
138 database are summarized in this section.

### 139 **2.1.1 the GPW Dataset**

140 Using the areal interpolation techniques, the Gridded Population of the World  
141 dataset, Version 4 (GPWv4), Revision 11, was constructed from national or subnational  
142 administrative units in conjunction with the most detailed spatial resolution available  
143 from the Population and Housing Censuses occurring in 2005 and 2014. After  
144 extrapolated to produce population estimates for the years 2000 to 2020 at a 5-year  
145 interval with a resolution of 30 arc-seconds (approximately 1 km at the equator), these  
146 estimates were further adjusted to national totals to consist of the United Nation's World  
147 Population Prospects (UN-WPP) adjusted population estimates and densities for those  
148 years. The GPW dataset includes estimates for 2000, 2005, 2010, 2015 and 2020  
149 respectively, and is freely accessible at  
150 <http://sedac.ciesin.columbia.edu/data/collection/gpw-v4>. The GPWv4 has provided  
151 globally consistent and spatially explicit disaggregated population data that is  
152 compatible with data set from other disciplines.

### 153 **2.1.2 the GRUMP dataset**

154 The Global Rural-Urban Mapping Project, Version 1 (GRUMPv1) dataset, which  
155 is based on GPWv3, has well identified urban area with observations of NOAA's NTL  
156 data collected over several decades. It differs from GPW by incorporating urban-rural  
157 reallocation of spatially distributed population in each census unit, and contains eight  
158 global data sets: population count, population density, urban settlement points, urban-  
159 extents, land/geographic unit area, national boundaries, national identifier, and



160 coastlines. GRUMPv1 provides global population estimates for 1990, 1995, and 2000  
161 at a resolution of 30 arc seconds (approximately 1 km at the equator) as well as at  
162 national, continental, and global scales at  
163 <https://sedac.ciesin.columbia.edu/data/set/grump-v1-population-density>. The GRUMP  
164 was the first global database that connects NTL images with population estimates, and  
165 helps better understand differences between urban and rural areas in terms of  
166 vulnerability, exposure, and resilience to environmental and climate change.

### 167 **2.1.3 the WorldPop dataset**

168 Growing from the AsiaPop, AfriPop, and AmeriPop population mapping projects,  
169 the WorldPop ([www.worldpop.org](http://www.worldpop.org)) was initiated in Oct 2013 and provided full open  
170 access archive of spatial demographic information around the world (Stevens et al.,  
171 2015; Tatem, 2017). Based on the random forest model and contemporary census data  
172 from hundreds of national statistics offices and other organizations, survey, remote  
173 sensing outputs and geospatial data etc., the WorldPop produces consistent gridded  
174 population density at 3 and 30 arc-seconds (about 100 m at the equator for individual  
175 countries, and about 1 km for the global mosaics, respectively). Then it was adjusted to  
176 match the official United Nations population estimates for 2000 to 2020 annually.  
177 Comparing with previous gridded population results, the WorldPop shows clear  
178 advantage in its method advancement, contemporary and easily-updatable consistent  
179 population distribution, characteristics and changes over time, enabling flexible  
180 integration with datasets on other types of geospatial data.

### 181 **2.1.4 the LandScan dataset**

182 The LandScan Global Population database from the Urban Oak Ridge National  
183 Laboratory, USA is a widely used population data set that developed using best  
184 available census and geographic data, remote sensing imagery analysis techniques  
185 within a multivariate dasymetric modeling framework to disaggregate census counts  
186 within an administrative boundary (Bhaduri et al., 2007). Commercial data was utilized



187 in LandScan for higher spatial accuracy in population allocation at 30 arc-seconds  
188 resolution for 1998, and 2000-2018 annually. The DN values represent population totals  
189 per grid cell. The global LandScan population data set is now available to the  
190 educational community free of charge at <https://landscan.ornl.gov/>, and has also been  
191 widely used in GDP disaggregation with fine reliability.

### 192 **2.1.5 census**

193 National and subnational (at state level) population totals around the global can be  
194 easily obtained from the World Bank. Meanwhile, census at county level for the U.S.  
195 and China were adopted from the U.S. Census Bureau and the Statistical Yearbook from  
196 National Bureau of Statistics, China (NBS) respectively, offering the flexibility to  
197 perform analysis at state (or provincial) and county levels.

198

## 199 **2.2 GDP**

200 The official GDP is usually collected at national scale, but it is often problematic  
201 to obtain data at a finer resolution (e.g., at state, city and county levels), especially in  
202 many developing countries (Nordhaus, 2011). Using NTL images and some other  
203 auxiliary data can help improve the quality of spatial allocation of GDP and offer a  
204 reliable substitution to conduct cross-disciplinary research a large literature.

### 205 **2.2.1 national and subnational GDP**

206 The World Development Indicators assembled by the World Bank (WB-WDI)  
207 provide a vast resource of relevant, high-quality, and internationally comparable  
208 socioeconomic statistics for 217 economies and more than 40 country groups which  
209 can be tracing back to more than 50 years. For most economies, GDP PPP (GDP  
210 converted using Purchasing Power Parity rates) values are extrapolated from the 2011  
211 International Comparison Program (ICP) benchmark estimates or imputed using a





212 statistical model based on the 2011 ICP. National GDP (in PPP) and GDP per capita  
213 (Pcap) figures in 2005: in current U.S. dollars and in current international dollars, were  
214 chosen and to be consistent with currency unit of GDP for SSP scenarios. For the  
215 meantime, national population totals are obtained from WB-WDI database as well.

216 Subnational GDP in 2005, 2010 and 2015 for the U.S. and China were obtained  
217 from departments of the U.S. Bureau of Economic Analysis and the Chinese National  
218 Bureau of Statistics, offering the flexibility to socioeconomic performance at state (or  
219 provincial), city and county levels. The Chinese GDP were obtained from the China  
220 Statistical Yearbooks, the China City Statistical Yearbooks, and the China County  
221 Statistical Yearbook with values recorded in RMB currency unit and then converted to  
222 USD using conversion factors provided from the World Bank.

### 223 **2.2.2 the NTL-based GDP**

224 The NTL images have shown well correlation with global and regional economic  
225 activities and been widely used to spatialize GDP data into a fine-scale (Ghosh et al.,  
226 2010; Nordhaus, 2011). The widely used version 4 DMSP-OLS stable NTL images for  
227 1992 - 2013 can be obtained from the National Oceanic and Atmospheric  
228 Administration's National Geophysical Data Center (NGDC) at  
229 <https://www.ngdc.noaa.gov/eog/dmsp/downloadV4composites.html>, with a spatial  
230 resolution of 30 arc-seconds and latitudinal and longitudinal extent from 75°N to 65°S  
231 and 180°W to 180°E. There are two separate annual stable NTL images derived from  
232 two sensors to avoid degradation problem, and each stable NTL image is a composition  
233 of all the available cloud-free data with background noises and ephemeral lights  
234 removed within this year. The DN values for DMSP-OLS stable NTL data range from  
235 0 to 63 with saturation problem (DN values of 63) scattered mainly in city centers and  
236 other brightly lit zones (Bennett and Smith, 2017). To improve the DMSP-OLS data  
237 quality, the new generation of NTL products, namely the Suomi-NPP-VIIRS Day/Night  
238 Band (DNB) images, were launched since 2012 with a higher resolution of 15 arc-  
239 seconds and a wider radiometric detection range. The Suomi-NPP-VIIRS DNB data



240 can be obtained from [https://eogdata.mines.edu/download\\_dnb\\_composites.html](https://eogdata.mines.edu/download_dnb_composites.html).

241 The NTL images have been widely used in spatial allocation of GDP at resolutions  
242 from  $500\text{ m} \times 500\text{ m}$  to  $1^\circ \times 1^\circ$  (Bennett and Smith, 2017; Nordhaus, 2011; Zhao et al.,  
243 2018). Based on the theory that national and sub-national GDP totals are directly  
244 distributed or regression related to each pixel in proportion to the DN values, global  
245 and regional NTL-based GDP can be spatialized into a fine-scale and integrated with  
246 data across disciplines (Chen et al., 2020; Ghosh et al., 2010; Zhao et al., 2017; Zhu et  
247 al., 2017).

248

### 249 **2.3 SSP projection data**

250 The long-term demographic and GDP projections have been promoted by different  
251 organizations to facilitate research on future impacts, adaptation, and vulnerability. The  
252 five SSPs (O'Neill et al., 2014), which are differentiated by different combinations of  
253 climate change mitigation and adaptation challenges, provide a wide range of  
254 information on possible global socioeconomic developments decennially up to 2100.  
255 SSP1 (“Sustainability”) characterizes a world shifting gradually but pervasively in a  
256 sustainable path with low mitigation and adaptation challenges, emphasizing more on  
257 human well-being than economic growth. SSP2 (“Middle of the Road”) follows a path  
258 of continuing historical trends associated with moderate income growth, facing medium  
259 challenges to mitigation and adaptation. SSP3 (“Regional Rivalry”) is characterized  
260 by slow economic growth with restriction of high mitigation and adaptation challenges.  
261 SSP4 (“Inequality”) represents a highly unequal world with high adaptation challenges,  
262 and economy growth rate inclines more to rich countries. Finally, SSP5 (“Fossil-fueled  
263 development”) characterizes a world of rapid economic growth with high mitigation  
264 challenges.

265



### 266 **2.3.1 SSP Database**

267       Based on harmonized assumptions for the interpretation of the SSP storylines in  
268 terms of the main drivers of economic growth, three sets of global GDP projections  
269 were provided in June 2013 in the SSP database. Recommended by the SSP database,  
270 the Organization for Economic Cooperation and Development (OECD) (Dellink et al.,  
271 2015) has developed a set of GDP projections based on different perspectives on future  
272 socioeconomic development, emphasizing on the key drivers of economic growth in  
273 the long run: population, total factor productivity, physical capital, employment and  
274 human capital, and energy and fossil fuel resources for 184 OECD countries up to the  
275 end of 21st century in 2005 USD in PPP for five SSP scenarios. The other two sets of  
276 GDP projections were developed by the International Institute for Applied Systems  
277 Analysis (IIASA) (Cuarema, 2015) for 144 countries, and the Potsdam Institute for  
278 Climate Impact Research (PIK) (Leimbach et al., 2015) for 32 world regions. These  
279 three sets of GDP projections are openly available from the SSP database hosted by the  
280 IIASA Energy Program at <https://tntcat.iiasa.ac.at/SspDb>.

281       The three sets of GDP projections were developed using the demographic  
282 projections to maintain consistency in assumptions with education and ageing but  
283 differed with respect to the employed drivers, methodology and outcomes, spanning a  
284 wide range broadly representative of the current literature, and inevitably subjecting to  
285 large uncertainties especially for the later decades (Riahi et al., 2017). A wide range of  
286 possible factors, like policy actions, external shocks, governance barriers, and  
287 feedbacks of greenhouse gas emission and climate extremes, are failed to predict and  
288 disregarded in the SSP framework. Whatsoever, these GDP projections do illustrate a  
289 substantial variance in global socioeconomic development and provide a basis for  
290 quantitative analyzing the climate change impacts on economic for each SSP (O'Neill  
291 et al., 2014; Riahi et al., 2017).

292       Together with the GDP projections, the long-term demographic projections (KC  
293 and Lutz, 2017) in the SSP database for each SSP scenario were developed by the IIASA  
294 and the National Center for Atmospheric Research (NCAR). Using a multidimensional



295 demographic model, national populations were projected based on alternative  
296 assumptions on future fertility, mortality, migration and educational transitions in each  
297 country for five SSPs (O'Neill et al., 2014; Riahi et al., 2017). The population  
298 projection can well capture the link between human capital and income growth in the  
299 econometric model as highlighted in the literature (KC and Lutz, 2017), and can also  
300 be accessed at <https://tntcat.iiasa.ac.at/SspDb>.

### 301 **2.3.2 population projection of 1/8 degree from SEDAC**

302 No doubt that the national projections in the SSP database failed to meet the  
303 increasing demand of spatially explicit demographic and GDP projections. Hence,  
304 Jones and O'Neill (Jones and O'Neill, 2016) have further extended the national totals  
305 and produced a scenario-based gridded population data set by downscaling the urban  
306 and rural population projections for each of the 232 countries to a spatial resolution of  
307  $1/8^\circ$  (approximately 7.5 arc-minutes at the equator). The gridded population from the  
308 GRUMP dataset in 2000 at a resolution of  $2.5'$  was used as the base-year population for  
309 future projection downscaling. Using the parameterized gravity model-based approach,  
310 the demographic driving factors, namely the current fertility, income, urbanization, and  
311 international migration are explicitly included in the population projections  
312 corresponding to each SSP and thus can reflect its spatial pattern as prescribed. The  
313 gridded population projections data set are quantitatively consistent with total, urban,  
314 rural populations at a national level at ten-year intervals for 2010-2100, and with  
315 urbanization projections as well as with the assumptions of SSP narratives.

316

### 317 **2.3.3 GDP projections from NIES, Japan**

318 Based on Jones and O'Neill, Murakami and Yamagata (2019) from the Center for  
319 Global Environmental Research, National Institute for Environmental Studies (NIES),  
320 Japan, have developed a new set of data by spatializing the national population and  
321 GDP into 0.5-degree grids for SSP1, SSP2 and SSP3. As described in Murakami and



322 Yamagata (2019), this gridded population projection data set trumps data from Jones  
323 and O'Neill by utilizing not only the urban and nonurban populations, but also taking  
324 the intensity of interactions among cities and auxiliary variables including road network,  
325 land cover, and location of airports into account. Among which, national urban  
326 populations are downscaled into cities based on a city growth model, and then used to  
327 project urban expansion/shrinkage with help of those auxiliary data. The GDP  
328 projections were then developed based on its populations at a spatial resolution of 0.5-  
329 degree for SSP1-3 only as well.

330 However, only two years data from settlement Points, v1 from GRUMP, SEDAC  
331 (<http://sedac.ciesin.columbia.edu/data/set/grump-v1-settlement-points>) were used in  
332 the city growth model parameterization and then in the future urban  
333 expansion/shrinkage projections (Murakami and Yamagata, 2019), which would raise  
334 some doubt on its credibility in these gridded population and GDP projections data sets.

#### 335 **2.3.4 Chinese Population Projections under two-children policy**

336 The implementation of two-children policy in 2016 and clear differences among  
337 the drivers (e.g., age, education enrollment in the historical period) between the NBS,  
338 China and the U.N. (Huang et al., 2019) require updates in Chinese population and GDP  
339 projections for all five SSPs. Since the demographic changes play a decisive role on  
340 future labor force and therefore affecting socioeconomic development, Jiang et al.  
341 (2017; 2018) have adopted data from China Statistical Yearbook and the Sixth National  
342 Population Census and made projections of Chinese population and GDP for 2020-2100  
343 based on assumptions of future fertility, mortality, and migration for each of five SSPs  
344 under two-children policy. Using the parameterized population-development-  
345 environment analysis model, Jiang et al. (2017) have implemented the population  
346 projections incorporating with national and provincial age, sex, and educational  
347 attainment that are quantitatively consistent with changes of birth rate under two-  
348 children policy in China. The provincial population projections were provided at a  
349 spatial resolution of 0.5-degree for five SSPs.



350 Chinese GDP (Jiang et al., 2018) were also projected using the total factor  
351 productivity, capital stock, and labor force etc., as input for five SSPs but not been  
352 utilized in this research.

353

### 354 **3 Method**

#### 355 **3.1 the official data interpolation**

356 National GDP PPP (in USD) for 2005 were obtained from the WB-WDI first for  
357 the 189 countries provided (data in China was for mainland only, and GDP in Hong  
358 Kong Special Administrative Region, Macao Special Administrative Region and  
359 Taiwan were divided but listed as individuals). For 36 island countries like British  
360 Virgin Islands, Cayman Islands, Cook Islands and etc., where GDP were unavailable  
361 from WB-WDI, data were obtained from the Central Intelligence Agency (CIA) World  
362 Factbook (released in 2015). GDP in Taiwan (China), Nauru, and Syrian Arab Republic  
363 were from the International Monetary Fund (IMF, released in Oct 2017). GDP for the  
364 rest 11 countries (namely Aland Islands, French Guiana, Holy See, Curacao, Bonaire  
365 Saint Eustatius and Saba, Norfolk Island, Pitcairn, Saint-Barthelemy, South Sudan,  
366 Svalbard and Jan Mayen Islands, and Tokelau) were set as zero where no data to be  
367 found. All GDP data were presented in PPP in 2005 USD using conversion factors  
368 provided from the World Bank.

369 Meanwhile, census data were also obtained to calculate GDP per capita in order to  
370 spatially allocate global GDP. National population totals in 2005 were obtained from  
371 the WB-WDI for 216 countries and regions. For the rest countries (regions) without  
372 available official census, data from other organizations were used instead. Population  
373 in Taiwan (China) was obtained from IMF. For Norfolk Island, Pitcairn, Saint-  
374 Barthelemy, Svalbard and Jan Mayen Islands, Guernsey, and Jersey, their population  
375 were obtained from CIA World Factbook. Mayotte, the Holy See, Cook Islands,  
376 Falkland Islands (Malvinas), French Guiana and others, 17 countries in total,



377 populations were obtained from the Wire & Plastic Products Group. Population in  
378 Aland Islands was obtained in ASUB National accounts since it is not provided in those  
379 global organizations.

380 The official GDP for China and the U.S. in 2005 were obtained the China Statistical  
381 Yearbooks and the BEA at state (or provincial) and county levels. GDP for 51 states  
382 and 3193 counties in the U.S., and for 31 provinces and 2326 counties with valid values  
383 in China were obtained for validation and further updates. Meanwhile, global census at  
384 state level (1865 states with valid values) were obtained from World Bank as well.

385

## 386 **3.2 population-based GDP disaggregation**

### 387 **3.2.1 baseline population selection**

388 The historical gridded population varies substantially since they differ in the  
389 reliability and variety of input data sources, the interpolation and decomposition  
390 methods of disaggregating national and subnational totals, the modeling approach, and  
391 how they cooperate with each other to determine population distribution. To choose  
392 more suitable gridded population as base map in GDP disaggregation, comparisons  
393 were made between national and subnational census against the gridded data sets from  
394 the GPWv4, the GRUMP, the WorldPop and the LandScan, which were spatially joined  
395 to the corresponding GIS-based administrative boundaries.

396 At national and state scales, the biases were all relatively small in 2005. The  $R^2$  are  
397 all approaching to 1.0 and averaged RMSE are 1.2, 4.1 and 5.1 million people for the  
398 GPWv4, World Pop and LandScan at national scale (Figure S1(a)). For 1565 states  
399 (provinces) around the globe, their  $R^2$  are around 0.98 and averaged RMSE are 1.7, 1.8  
400 and 1.8 million, respectively (Figure S1(b)). Further comparison of 3193 counties in  
401 the U.S. in four selected years: 2000, 2005, 2010 and 2015 showed that,  $R^2$  are all  
402 around 0.95 and their slope are approximately 0.99 including about 200 specific  
403 counties with clear biases population totals. This is obvious since the openly available



404 census are the primary input in constructing these gridded data sets.

405

406 <Figure 1>

407

408 Comparisons at county level in China for the years of 2000 (1870 out of 2345  
409 counties with valid values), 2005 (1874 counties), 2010 (1923 counties) and 2015 (1801  
410 counties) (Figure 1) show that the LandScan outperformed in its accuracy with  $R^2$   
411 slightly higher and RMSE relatively smaller, approximately two thirds of RMSE from  
412 the GPWv4 and the WorldPop (Figure 1). This shows that the LandScan can well  
413 estimate population redistribution at county level than GPWv4 and WorldPop, and  
414 therefore recommended as base map in spatial allocation of global GDP.

### 415 3.2.2 Population Based GDP disaggregation

416 Population can well capture the link between human capital and income growth in  
417 the econometric model, and broad literature has emphasized the role of human capital  
418 as a key driver of economic growth (Cuarema, 2015; Dellink et al., 2015; KC and Lutz,  
419 2017). Shioyama et al. (2011) have suggested the robustness of an ensemble learning-  
420 based downscaling approach, which are defined by (baseline variable)  $\times$  (control  
421 variable) in accordance with distribution weights. This approach can be applied in  
422 spatial allocation of global GDP based on the LandScan population ( $Pop_{pixel}$ , as baseline  
423 variable) and GDP per capital ( $Pcap$ , ratio of GDP to population totals in a given  
424 administrative boundary  $i$ , as control variable) to 1 km  $\times$  1 km grids (denote  $GDP_{Pop}$ ).

$$425 \quad GDP_{Pop} = Pop_{pixel} \times Pcap = Pop_{pixel} \times \frac{GDP_i}{Pop_i} \quad (1)$$

426





### 427 **3.3 NTL involved GDP disaggregation**

#### 428 **3.3.1 NTL-based GDP disaggregation**

429 The satellite-derived NTL data has been proven to correlate well with GDP at all  
430 examined scales and has been widely used in spatial allocation of GDP over large areas  
431 (Ghosh et al., 2010; Nordhaus, 2011). The DMSP-OLS NTL images in 2005 (average  
432 visible, stable lights, and cloud free coverages, satellites F14 and F15 simultaneously  
433 collected global NTL images and data from F15 was chosen as newer sensor would  
434 have less degradation of data quality) have been utilized to disaggregate global GDP to  
435 a spatial resolution of 30 arc seconds. Based on the theory that the GDP totals are  
436 directly distributed to each pixel in proportion to the DN values in a given  
437 administrative boundary, the NTL-Based GDP disaggregation (denoted  $GDP_{NTL}$ ) can  
438 be described as,

$$439 \quad GDP_{NTL} = GDP_{per\_light} \times DN_{pixel} = \frac{GDP_i}{SL_i} \times DN_{pixel} \quad (2)$$

440 where  $GDP_i$  is the GDP totals,  $SL_i$  is the sum of DN values and  $GDP_{per\_light}$  is the  
441 constant in administrative unit  $i$ ,  $DN_{pixel}$  and  $GDP_{pixel}$  are the DN value and  
442 corresponding GDP in each pixel in administrative unit  $i$ .

#### 443 **3.3.2 NTL & population based GDP disaggregation**

444 The saturation problem in the DMSP-OLS NTL images, however, has resulted in  
445 overestimation in urban centers and underestimation in rural and distanced areas. Zhao  
446 et al., (2017) have improved its accuracy by incorporating the gridded population data  
447 into NTL-based GDP disaggregation in each pixel since population data has an  
448 exponential relationship with DN values of NTL images. By multiplying the NTL  
449 image with the LandScan population data in 2005, Lit-Pop image was produced and  
450 then used in Equation 3 to spatialize GDP at global scale (denoted  $GDP_{Lit-Pop}$ ):

$$451 \quad GDP_{Lit-Pop} = \frac{GDP_i}{SLP_i} \times DN_{lp} \quad (3)$$

452 where  $DN_{lp}$  is the DN value of each pixel of Lit-Pop data, and  $SLP_i$  is the sum of the



453 DN values of Lit-Pop image in administrative unit  $i$ .

454

### 455 **3.4 Historical GDP disaggregation**

456 To examine the performance of three GDP disaggregation approaches above,  
457 namely the  $GDP_{Pop}$ ,  $GDP_{NTL}$  and  $GDP_{Lit-Pop}$ , national GDP in China and U.S. from WB-  
458 WDI instead of official state or county values were used to spatialize global interpolated  
459 official GDP into  $1\text{ km} \times 1\text{ km}$  grid using the global LandScan population, DMSP-OLS  
460 NTL images in 2005. Meanwhile, GDP PPP (in 2005 USD) from 52 states in USA plus  
461 31 provinces in China, 321 cities in China, and 3068 plus 2091 counties in USA and  
462 China in 2005 have been adopted and spatially joined to the corresponding GIS-based  
463 administrative boundaries respectively, and used to verify the disaggregated GDP  
464 results.

465

466 <Figure 2>

467

468 The comparisons showed that the accuracy of three disaggregated GDP decreases  
469 accompanied by the changes of their spatial scales, and  $GDP_{NTL-Pop}$  is superior to  
470  $GDP_{Pop}$  and  $GDP_{NTL}$  at national, state (provincial), and county levels with clear  
471 advantages evaluated by their  $R^2$  and RMSE. In detail,  $GDP_{Lit-Pop}$  can better identify the  
472 spatially allocated GDP at finer spatial scales with higher accuracy with  $R^2$  reaching  
473 0.78 and RMSE of 8.35 billion USD for 5221 counties in the U.S. and China. While the  
474  $R^2$  is only 0.47 and RMSE reaches as high as 14.34 billion between official GDP and  
475  $GDP_{NTL}$ , indicating less advantageous due to the saturation problem.

476 Meanwhile, GDP using the global LandScan population only as base map ( $GDP_{Pop}$ )  
477 can well identify GDP redistribution at finer spatial scales as well. The  $R^2$  between  
478 official GDP and  $GDP_{Pop}$  at county level in the U.S. and China reaches as high as 0.73  
479 and the averaged RMSE is 9.80 billion USD in 2005, which performs better than  
480  $GDP_{NTL}$  and is nearly comparable to  $GDP_{Lit-Pop}$ , indicating that  $GDP_{Pop}$  can be used as



481 an alternative when  $GDP_{Lit-Pop}$  is limited.

482 Similar results can be obtained in 2015 as another validation case when using the  
483 NPP-VIIRS NTL images, the global LandScan population and official GDP (Figure S2).  
484 National GDP from WB-WDI were used in GDP disaggregation, and subnational GDP  
485 from the U.S. Census Bureau and the corresponding Statistical Yearbooks in China  
486 were used for validation purpose.  $GDP_{Lit-Pop}$  outperformed with higher  $R^2$  of 0.96 in 52  
487 states in U.S. plus 31 provinces in China, and their RMSE (90.39 billion USD) is about  
488 one-half of that of  $GDP_{Pop}$ , and only one-third of  $GDP_{NTL}$ , showing clear advantage in  
489 spatial allocation of GDP at a medium spatial scale. Meanwhile,  $GDP_{Pop}$  and  $GDP_{Lit-Pop}$   
490 both outperformed than  $GDP_{NTL}$  at county level, and  $GDP_{Pop}$  even performs a slightly  
491 superior with smaller RMSE of 14.11 billion USD than  $GDP_{Lit-Pop}$  (RMSE of 15.36  
492 billion USD) (Figure S2).

493

494 All above showed that population involved base map can be used in spatial  
495 allocation of GDP as well. The  $GDP_{Lit-Pop}$  is recommended for global, state and county  
496 scales disaggregation, and  $GDP_{Pop}$  can be used as an alternative and especially at county  
497 or even smaller scales where NTL images are limited in very rural regions.

498 Based on above, we updated official GDP and GDP per capita (in PPP) at county  
499 level in the U.S. and China, and then disaggregated the global GDP in 2005 into 1 km  
500  $\times$  1 km grid based on the NTL images and the LandScan population together as base  
501 map to ensure spatial accuracy. This gridded GDP PPP in 2005 was used as historical  
502 gridded GDP in the following comparison.  $GDP_{Pop}$  in 2005 was also provided.

503

### 504 **3.5 Global GDP downscaling for SSPs**

505 NTL image projections for future scenarios are off limits and therefore unavailable  
506 for spatial allocation of GDP for different SSP scenarios. Luckily, a set of global  
507 spatially explicit population projections that are consistent with SSPs was developed  
508 with a spatial resolution of 0.125 degree (Jones and O'Neill, 2016), which can be used



509 in spatial allocation of GDP projections to a spatial resolution of 0.125 degree first using  
510 the above  $GDP_{Pop}$  approach. Assuming that there will be no population mobility and  
511 such within countries and across the grids, the GDP projections can be further  
512 downscaled to 1 km  $\times$  1 km grids using NTL images and global LandScan population  
513 in 2015 as fixed base map.

514 First, we completed the GDP and population projections for all the countries  
515 (regions) in the SSP database. Population projections from IIASA were adopted since  
516 its historical data in 2005 were less biased with  $R^2$  approaching 1.0 and averaged bias  
517 of 0.27% for 178 countries when compared against national population totals from WB-  
518 WDI data set. Population (GDP) projections for 182 (177) countries were obtained from  
519 IIASA (OECD, as recommended) in the SSP database. Meanwhile, the supranational  
520 projections for the rest countries where the associated world regions the countries  
521 belong to were obtained and filled to complete the future time series to ensure the  
522 consistency for all five SSP scenarios.

523 Next, we recalculated the GDP per capital. Instead of using the exact GDP (PPP in  
524 2005 USD), population, and GDP per capital predictions directly since these values  
525 vary greatly among different originations, GDP per capita growth rate relative to that  
526 in 2005 (provided from SSP database) were obtained for each country. The new national  
527 GDP per capita for all five SSPs were recalculated by multiplying these growth rates  
528 with GDP per capita settled (based on the WB-WDI) for 2005. Meanwhile, extra  
529 arrangement was set for the following countries. To be more specific, in Pitcairn, Saint  
530 Helena, Svalbard and Jan Mayen Islands, and Tokelau, the national GDP per capital  
531 growth rate were set as 1.0 (constants for future scenarios due to missing predictions)  
532 for all five SSPs. The Somalia's GDP per capita growth rate was assumed to follow that  
533 of the African region since its GDP was missing in 2005. Furthermore, GDP per capital  
534 growth rate in Switzerland and Sudan were used to replace the values in Liechtenstein  
535 and South Sudan instead of the regional data due to geopolitical reason.

536 Then we disaggregate the global GDP projections using  $GDP_{Lit-Pop}$  approach. We  
537 first updated Chinese population in the gridded population of 1/8 degree from SEDAC



538 with population projections developed by Jiang et al., (2017) under two-children policy  
539 in China, which were downscaled to a spatial resolution of 0.125 degree for all five  
540 SSPs. After national and regional GDP per capita recalculated by utilizing the above  
541 GDP per capita, and spatially joined to the corresponding administrative boundaries,  
542 national GDP were preliminary redistributed by multiplying with scenario-based global  
543 population projections (Jiang et al., 2017; Jones and O'Neill, 2016) with a spatial  
544 resolution of  $1/8^\circ$  for 2030-2100 at 10-year intervals for all five SSPs using the  $GDP_{Pop}$   
545 approach. The DMSP-OLS stable NTL data in 2013 was adopted to replace the negative  
546 DN values from the Suomi-NPP-VIIRS DNB images in 2015. After resampled to a  
547 spatial resolution of 1 km, the global LandScan population in 2015 were introduced to  
548 calculate the base map. Following the  $GDP_{Lit-Pop}$  approach, the preliminary  
549 redistributed GDP at  $1/8^\circ$  resolutions were further disaggregated to a spatial resolution  
550 of 30 arc seconds ( $\sim 1$  km) for all five SSPs, using Lit-Pop in 2015 as fixed spatially  
551 explicit pattern of GDP. Spatially explicit global GDP in 2005 and in 2030, 2050, and  
552 2100 (as representative) are shown in Figures 3-5 to present substantial long-term  
553 changes of GDP under five SSP scenarios.

554

555 <Figure 3>

556 <Figure 4>

557 <Figure 5>

558

559 Last, we disaggregate the global GDP using LandScan population only as base map  
560 as an alternative choice. Following the same procedure, the LandScan global population  
561 in 2018 (latest obtained) was used as base map, and the above preliminary global GDP,  
562 which were downscaled to a spatial resolution of  $1/8^\circ$  for 2030-2100 at 10-year intervals  
563 for all five SSPs with Chinese GDP projections updated under the two-children policy,  
564 were disaggregated to  $1\text{ km} \times 1\text{ km}$  grids (2030, 2050, and 2100 as representative and  
565 shown in Figure S6-S8). The GDP projections based on  $GDP_{Pop}$  approach can be used  
566 as an alternative when NTL images are limited in very rural regions or at a finer spatial



567 scale.

568 It is worth mentioning that the LandScan population data set was used as base map  
569 as an alternative in GDP disaggregation as 1) using population data set as base map  
570 performs no worse than that of  $GDP_{Lit-Pop}$  (Figure 2), and 2) valid values only exists  
571 when the original NTL images and population were both not null in Lit-Pop, and that  
572 may result in some overestimation in city area.

573

#### 574 **4 Result**

575 Consistent with the national totals in the SSP database and the SSP narratives,  
576 global and regional GDP depict different patterns among different SSP scenarios. The  
577 highest GDP projection will reach more than 21 times in SSP5 while the lowest  
578 projection only stays around 4.4 times in SSP3 that of 2005 by 2100 at global scale.  
579 Visible differentiations appear around 2060 with averaged about 4.9 times that of 2005  
580 but expand to about 4.4 - 12.8 times by 2100 for SSP1-SSP4 globally. GDP in all five  
581 SSPs depict varying degrees of development with a slowing down in GDP growth rates  
582 over time, especially in the second half century in most developing countries.  
583 Meanwhile, GDP projections vary greatly across nations but are mainly consistent with  
584 the national GDP growth rate projections from the SSP database. For example, GDP in  
585 the U.S. expands only about 4.8 times in SSP5 and to about 2.2 times in SSP3 that of  
586 2005 by 2100.

587 By replacing with two-children policy, the GDP projections in China, however, has  
588 led to different growing pattern among SSP scenarios. It exhibits a persistent increasing  
589 trend with highest of about 9.7 - 40.6 times that of 2005 by 2100 for all five SSP. While  
590 GDP projection from the SSP database shows a rapid development with a peak of  
591 around 2070-2080 for SSP1 and SSP3-5 with highest rates of about 7.1 - 18.7 times  
592 that of 2005 and then declined to about 6.9 - 18.1 times by 2100. These differences of  
593 Chinese GDP are result from the change of population due to the two-children policy,



594 which are predicted to continue growing with a peak of approximately 1.39 - 1.45  
595 billion around 2030, and then to decline under four SSPs with the exception of SSP3  
596 (Jiang et al., 2017), against the continue growing with a peak of 1.36 - 1.40 billion  
597 around 2030 and then to decline under all five SSPs in the SSP database.

598 The regional GDP also depicts major differences inequality. Taking Northeast  
599 America (including Virginia, West Virginia, Pennsylvania, Connecticut, Delaware,  
600 Maryland, New Jersey, New York, and District of Columbia), five countries in Europe  
601 (including Netherlands, Germany, Belgium, France, and Luxembourg), and Circum-  
602 Bohai Sea Region in China (including Beijing, Tianjin, Hebei, Liaoning, and Shandong  
603 provinces) as case study since these three regions share similar latitude, highly  
604 developed, and are densely populated areas. Their GDP vary substantially among  
605 different SSP scenarios as well as among different regions over time (Figure 6), with  
606 highest growth rate reaching about 5.3, 5.2, and 39.2 times (in SSP5) but lowest of  
607 about 2.4, 2.5, and 9.4 times (in SSP3) that of 2005 by 2100 for five countries in Europe,  
608 Northeast America and the Circum-Bohai region in China, respectively. European  
609 region and Northeast America show similar GDP growth rate over time, and the city  
610 centers and places along traffic show much higher GDP (about 50 to 100 billion USD  
611 in per grid) than rural regions (less than 5 billion) in these three regions (Figure 6).

612

613 <Figure 6>

614

## 615 **5 Data availability**

616 There are two sets of global GDP (PPP in 2005 USD to enable comparison among  
617 years and across regions) disaggregation results for 2005 as historical period and for  
618 2030-2100 as future projections for SSP1-5 at 10-year interval provided, one with Lit-  
619 Pop in 2015 as base map and the other using LandScan population in 2018 as base map.  
620 The two data sets are provided in “tif” format with a spatial resolution of 30 arc-seconds  
621 (approximately 1 km at the equator). The global GDP are disaggregated within its



622 administrative boundaries, and therefore the Antarctica, oceans as well as some desert  
623 or wilderness areas are filled with value 0. The spatial extents are 65S-75N and 180E-  
624 180W (limited due to the Suomi-NPP-VIIRS NTL image extent), and 55.875S-83.65N  
625 and 180E~180W in standard WGS84 coordinate system for two data sets, respectively.

626 The detailed information regarding to these GDP disaggregation results is available  
627 from “Global dataset of gridded GDP scenarios”, which is provided by the Global  
628 Change Risk of Population and Economic Systems (GCR-PES): Mechanisms and  
629 Assessments Project, Beijing Normal University, Beijing, China  
630 (<http://gcr.bnu.edu.cn/>). The two sets of gridded GDP projections are available at  
631 <https://doi.org/10.5281/zenodo.4350027> (Wang and Sun, 2020).

632

## 633 **6 Discussion and conclusion**

634 In this study, we produced a set of spatially explicit global GDP, which to the best  
635 of our knowledge, the first data set that presents substantial long-term changes of GDP  
636 for both historical period (2005 as representative) and for future projections under all  
637 five SSP scenarios with a spatial resolution of 1 km. The combination of gridded  
638 population and NTL images outperformed in GDP disaggregation across the globe, and  
639 official census and GDP in U.S. and China at county level were incorporated within  
640 GDP disaggregation. Chinese population in SSP database were replaced by Jiang et al.,  
641 (2017) which incorporates data from China Statistical Yearbook and the Sixth National  
642 Population Census at provincial scale and may offer a higher precision, and then used  
643 to spatialize GDP under two-children policy. The main objective is to provide a set of  
644 spatially explicit global GDP projections that is readily applicable across disciplines,  
645 and  $GDP_{Lit-Pop}$  is recommended at national, state and county scales, while  $GDP_{Pop}$  is  
646 recommended at county or even smaller scales where NTL images are limited in very  
647 rural regions.

648 However, this GDP dataset was bound to the national and subnational data of  
649 various data sources, and to the approaches including using uniformed national GDP





650 per capita growth rate within a country, using fixed gridded population and NTL images  
651 in specific historical year as base map for future GDP disaggregation, and etc.

652 First, the national and super-national population and GDP in SSP database are  
653 highly depend on the methodology used in projection, including the model, the input  
654 drivers, and assumptions of future developments, leading to varying projections from  
655 different global organizations. Similar to the vast majority of literatures, the effect of  
656 financial crisis and climate change policies, scientific and technological progress, and  
657 many political and societal factors are, however, in absence beyond those in place when  
658 data was developed for GDP disaggregation. The climate system feedbacks are not  
659 considered on GDP disaggregation for five SSPs as well. The uncertainties for original  
660 SSP projections, especially where data coverage is limited, also exist in this  
661 disaggregated GDP and should be treated with caution.

662 Second, using fixed spatial distribution of gridded population and NTL images at  
663 historical level as base map is based on the assumption that population mobility within  
664 countries and across the grids will not occur, thus the gridded GDP projections fail to  
665 capture the future spatial differences caused by population migration. Meanwhile, the  
666 DN value of zero in either gridded population or NTL images (e.g., regions like farther  
667 north of 65N or very rural places) can directly cause zero proportion of GDP, resulting  
668 in some bias in such regions (GDP downscaling using the LandScan population as only  
669 base map is recommended as an alternative).

670 Last, simple approach of using uniform national GDP per capita growth rate within  
671 a country to downscale the national GDP to match the future population totals at 0.125  
672 degree, can cause an even distribution of GDP in space, and is highly correlated with  
673 projected population distribution. Other inevitable shortages in this approach, like using  
674 the existing data that are combined with various techniques to replace missing values  
675 for future scenarios, the currency conversion factors used at national scale and etc., are  
676 no doubt adding more uncertainly in both historical and future GDP disaggregation.

677 Despite various known shortcomings and uncertainties that discussed above, this  
678 gridded GDP data set can provide a chance to allow for comparability of global and  
679 regional socioeconomic changes between historical period and future projections under



680 different socioeconomic development pathways as described by the SSPs. It can also  
681 broaden the applicability of regional economic activities and potentially feed back to  
682 climate impact research. Our results highlight the necessity and availability of using  
683 gridded GDP projections with high resolution, especially in hazard exposure,  
684 vulnerability, and resilience analysis for the ScenarioMIP research.

685

#### 686 **Author contributions.**

687 TW and FS designed the research, and TW performed the analysis and drafted the  
688 manuscript; FS provided insights on data product characteristics and underlying  
689 procedures.

690

#### 691 **Competing interests.**

692 The authors declare that they have no conflict of interest.

#### 693 **Acknowledgements**

694 This research was supported by the National Key Research and Development  
695 Program of China (2016YFA0602402, 2019YFA0606903), the TopNotch Young  
696 Talents Program of China (Fubao Sun), China Postdoctoral Science Foundation funded  
697 project (2018M640173, 2020T130646) and the National Natural Science Foundation  
698 of China (42001031).

699

#### 700 **Reference**

701 B. Merz, H. Kreibich, R. Schwarze, and Thielen, A.: Assessment of economic flood  
702 damage, *Natural Hazards and Earth System Sciences*, 10, 1697–1724, 2010.

703 Bennett, M. M. and Smith, L. C.: Advances in using multitemporal night-time lights  
704 satellite imagery to detect, estimate, and monitor socioeconomic dynamics,



- 705 Remote Sensing of Environment, 192, 176-197, 2017.
- 706 Bhaduri, B., Bright, E., Coleman, P., and Urban, M. L.: LandScan USA: a high-  
707 resolution geospatial and temporal modeling approach for population distribution  
708 and dynamics, *GeoJournal*, 69, 103-117, 2007.
- 709 Chen, J., Liu, Y., Pan, T., Liu, Y., Sun, F., and Ge, Q.: Population exposure to droughts  
710 in China under 1.5 °C global warming target, *Earth System Dynamics*, 2017. 1-13,  
711 2017.
- 712 Chen, Q., Ye, T., Zhao, N., Ding, M., and Yang, X.: Mapping China's regional economic  
713 activity by integrating points-of-interest and remote sensing data with random  
714 forest, *Environment and Planning B Urban Analytics and City Science*, 3. 1-19,  
715 2020.
- 716 Cuaresma, J. C.: Income Projections for Climate Change Research: A Framework  
717 Based on Human Capital Dynamics, *Global Environmental Change*, 42, 226-236,  
718 2015.
- 719 Dellink, R., Chateau, J., Lanzi, E., and Magné, B.: Long-term economic growth  
720 projections in the Shared Socioeconomic Pathways, *Global Environmental Change*,  
721 42. 200-214, 2015.
- 722 Doll, C. N. H., Muller, J. P., and Morley, J. G.: Mapping regional economic activity  
723 from night-time light satellite imagery, *Ecological Economics*, 57, 75-92, 2006.
- 724 Ghosh, T., L Powell, R., D Elvidge, C., E Baugh, K., C Sutton, P., and Anderson, S.:  
725 Shedding light on the global distribution of economic activity, *The Open*  
726 *Geography Journal*, 3, 2010.
- 727 Huang, J., Qin, D., Jiang, T., Wang, Y., Feng, Z., Zhai, J., Cao, L., Chao, Q., Xu, X.,  
728 and Wang, G.: Effect of Fertility Policy Changes on the Population Structure and  
729 Economy of China: from the Perspective of the Shared Socioeconomic Pathways,  
730 *Earths Future*, 7. 250-265, 2019.
- 731 IPCC: Climate change 2013: the physical science basis: Working Group I contribution  
732 to the Fifth assessment report of the Intergovernmental Panel on Climate Change,  
733 Cambridge University Press, Cambridge, U. K., 2014.
- 734 Jiang, T., Zhao, J., Cao, L., Wang, Y., Su, B., Jing, C., Wang, R., and Gao, C.: Projection



735 of national and provincial economy under the shared socioeconomic pathways in  
736 China, *Climate Change Research*, 14, 50-58, 2018.

737 Jiang, T., Zhao, J., Jing, C., Cao, L., Wang, Y., Sun, H., Wang, A., Huang, J., Su, B., and  
738 Wang, R.: National and Provincial Population Projected to 2100 Under the Shared  
739 Socioeconomic Pathways in China, *Climate Change Research*, 13, 128-137, 2017.

740 Jones, B. and O'Neill, B. C.: Spatially explicit global population scenarios consistent  
741 with the Shared Socioeconomic Pathways, *Environmental Research Letters*, 11,  
742 084003, 2016.

743 Jones, B., O'Neill, B. C., Mcdaniel, L., Mcginnis, S., Mearns, L. O., and Tebaldi, C.:  
744 Future population exposure to US heat extremes, *Nature Climate Change*, 5, 592-  
745 597, 2015.

746 KC, S. and Lutz, W.: The human core of the shared socioeconomic pathways:  
747 Population scenarios by age, sex and level of education for all countries to 2100,  
748 *Global Environmental Change*, 42, 181-192, 2017.

749 Kumm, M., Taka, M., and Guillaume, J. H.: Gridded global datasets for gross domestic  
750 product and Human Development Index over 1990–2015, *Scientific data*, 5,  
751 180004, 2018.

752 Leimbach, M., Kriegler, E., Roming, N., and Schwanitz, J.: Future growth patterns of  
753 world regions – A GDP scenario approach, *Global Environmental Change*, 42,  
754 2015.

755 Leyk, S., Gaughan, A. E., Adamo, S. B., Sherbinin, A. D., and Pesaresi, M.: The spatial  
756 allocation of population: a review of large-scale gridded population data products  
757 and their fitness for use, *Earth System Science Data*, 11, 2019.

758 Murakami, D. and Yamagata, Y.: Estimation of gridded population and GDP scenarios  
759 with spatially explicit statistical downscaling, *Sustainability*, 11, 1-18, 2019.

760 Nordhaus, C. W. D.: Using luminosity data as a proxy for economic statistics,  
761 *Proceedings of the National Academy of Sciences of the United States of America*,  
762 108, 8589-8594, 2011.

763 O'Neill, B. C., Tebaldi, C., Van Vuuren, D. P., Eyring, V., Friedlingstein, P., Hurtt, G.,  
764 Knutti, R., Kriegler, E., Lamarque, J.-F., and Lowe, J.: The scenario model



765 intercomparison project (ScenarioMIP) for CMIP6, Geoscientific Model  
766 Development, 9, 3461–3482, 2016.

767 O’Neill, B. C., Kriegler, E., Riahi, K., Ebi, K. L., Hallegatte, S., Carter, T. R., Mathur,  
768 R., and van Vuuren, D. P.: A new scenario framework for climate change research:  
769 the concept of shared socioeconomic pathways, Climatic change, 122, 387–400,  
770 2014.

771 Riahi, K., Van Vuuren, D. P., Kriegler, E., Edmonds, J., O’neill, B. C., Fujimori, S.,  
772 Bauer, N., Calvin, K., Dellink, R., and Fricko, O.: The shared socioeconomic  
773 pathways and their energy, land use, and greenhouse gas emissions implications:  
774 an overview, Global Environmental Change, 42, 153–168, 2017.

775 Shiogama, H., Emori, S., Hanasaki, N., Abe, M., Masutomi, Y., Takahashi, K., and  
776 Nozawa, T.: Observational constraints indicate risk of drying in the Amazon basin,  
777 Nature Communications, 2, 1–7, 2011.

778 Stevens, F. R., Gaughan, A. E., Linard, C., and Tatem, A. J.: Disaggregating census data  
779 for population mapping using random forests with remotely-sensed and ancillary  
780 data, PloS one, 10, 2015.

781 Su, B., Huang, J., Fischer, T., Wang, Y., Kundzewicz, Z. W., Zhai, J., Sun, H., Wang,  
782 A., Zeng, X., and Wang, G.: Drought losses in China might double between the 1.5  
783 C and 2.0 C warming, Proceedings of the National Academy of Sciences, 115,  
784 10600–10605, 2018.

785 Tatem, A. J.: WorldPop, open data for spatial demography, Scientific data, 4, 1–4, 2017.

786 Tobias, G.: Continuous national gross domestic product (GDP) time series for 195  
787 countries: past observations (1850–2005) harmonized with future projections  
788 according to the Shared Socio-economic Pathways (2006–2100), Earth System  
789 Science Data, 10, 847–856, 2018.

790 Wang, T., and Sun, F.: Spatially explicit global gross domestic product (GDP) data set  
791 consistent with the Shared Socioeconomic Pathways, zenodo, Dataset,  
792 <https://doi.org/10.5281/zenodo.4350027>.version 1, 2020.

793 Wang, X., Rafa, M., Moyer, J., Li, J., Scheer, J., and Sutton, P.: Estimation and mapping  
794 of sub-national GDP in Uganda using NPP-VIIRS imagery, Remote Sensing, 11,



795           2019.  
796   Wilbanks, T. J. and Ebi, K. L.: SSPs from an impact and adaptation perspective,  
797           Climatic change, 122, 473-479, 2014.  
798   Winsemius, H. C., Aerts, J. C., Van Beek, L. P., Bierkens, M. F., Bouwman, A., Jongman,  
799           B., Kwadijk, J. C., Ligtoet, W., Lucas, P. L., and Van Vuuren, D. P.: Global drivers  
800           of future river flood risk, Nature Climate Change, 6, 381-385, 2016.  
801   Zhao, N., Cao, G., Zhang, W., and L., S. E.: Tweets or nighttime lights: Comparison for  
802           preeminence in estimating socioeconomic factors, ISPRS Journal of  
803           Photogrammetry and Remote Sensing, 146, 1-10, 2018.  
804   Zhao, N., Liu, Y., Cao, G., Samson, E. L., and Zhang, J.: Forecasting China's GDP at  
805           the pixel level using nighttime lights time series and population images, Mapping  
806           ences & Remote Sensing, 54, 407-425, 2017.  
807   Zhu, X., Mingguo, M., Hong, Y., and Ge, W.: Modeling the Spatiotemporal Dynamics  
808           of Gross Domestic Product in China Using Extended Temporal Coverage  
809           Nighttime Light Data, Remote Sensing, 9, 626, 2017.

810  
811

## 812 **Figure Captions:**

813   Figure 1 Comparisons between official census and the gridded extractions from global  
814   population data sets for the years 2000 (a), 2005 (b), 2010 (c) and 2015 (d) at county  
815   level in China.

816

817   Figure 2 Comparison between official and disaggregated GDP at national level (a), and  
818   at state (b) and county (c) levels in U.S. and China in 2005, values in brackets are the  
819   RMSE.

820

821   Figure 3 The spatial allocation of global GDP using  $GDP_{Lit-Pop}$  approach for 2005 (a)  
822   and 2030 under SSP1-5 scenarios (b-f) at a spatial resolution of 1 km.



823

824 Figure 4 The spatial allocation of global GDP using  $GDP_{Lit-Pop}$  approach for 2005 (a)  
825 and 2050 under SSP1-5 scenarios (b-f) at a spatial resolution of 1 km.

826

827 Figure 5 The spatial allocation of global GDP using  $GDP_{Lit-Pop}$  approach for 2005 (a)  
828 and 2100 under SSP1-5 scenarios (b-f) at a spatial resolution of 1 km.

829

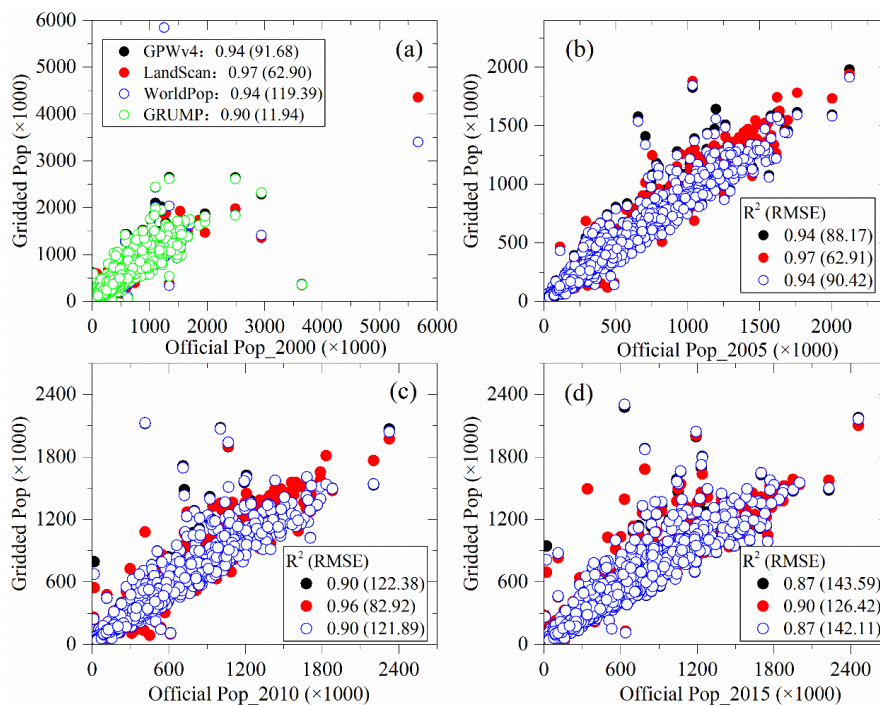
830 Figure 6 The spatial allocation of GDP in selected regions (Northeast America (a series),  
831 five countries in Europe (b series), and Circum-Bohai Sea Region in China (c series))  
832 for 2005 as historical period and for 2030, 2050, and 2100 using  $GDP_{Lit-Pop}$  approach  
833 under SSP1 scenario as study case (1 km resolution). Their spatial distribution and  
834 corresponding regional GDP growth (times that of 2005) are in the bottom.

835

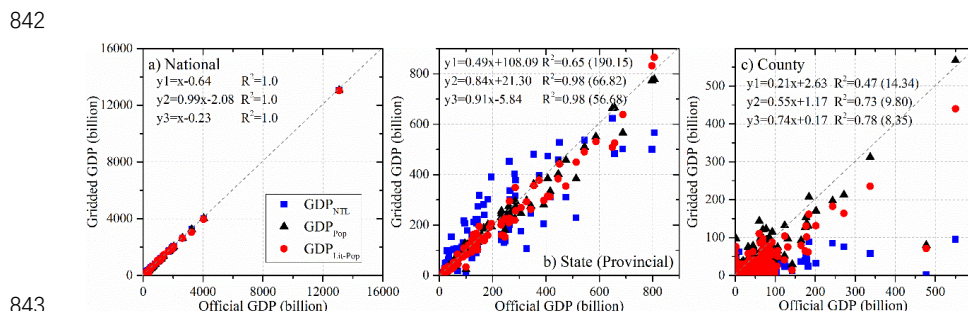
836



837 **Figure**



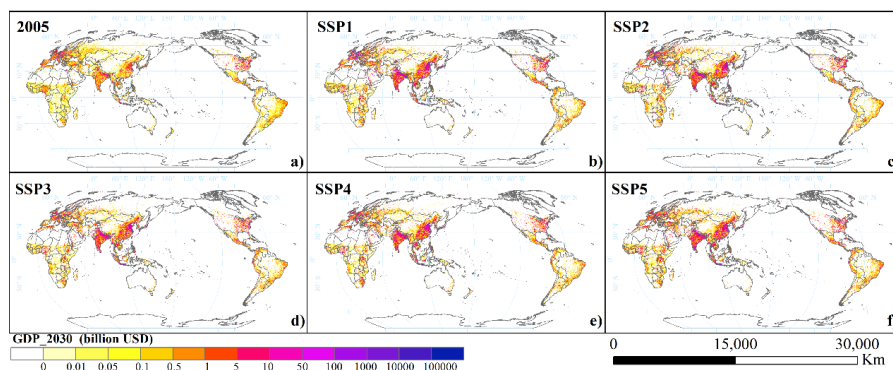
838  
 839 **Figure 1** Comparisons between official census and the gridded extractions from global  
 840 population data sets for the years 2000 (a), 2005 (b), 2010 (c) and 2015 (d) at county  
 841 level in China.



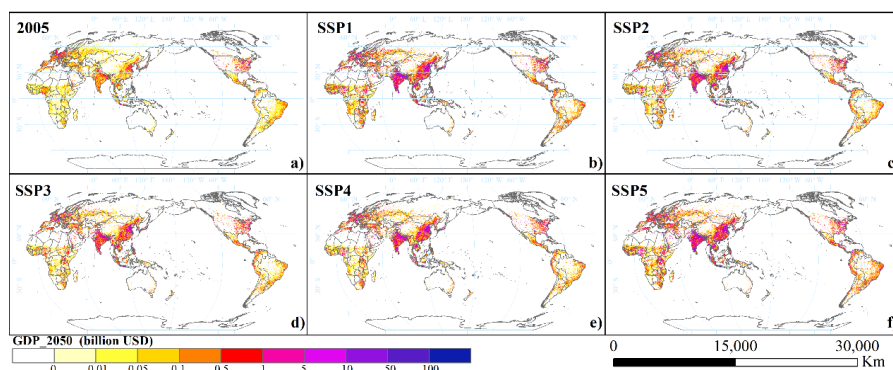
843  
 844 **Figure 2** Comparison between official and disaggregated GDP at national level (a), and  
 845 at state (b) and county (c) levels in U.S. and China in 2005, values in brackets are the  
 846 RMSE.

847

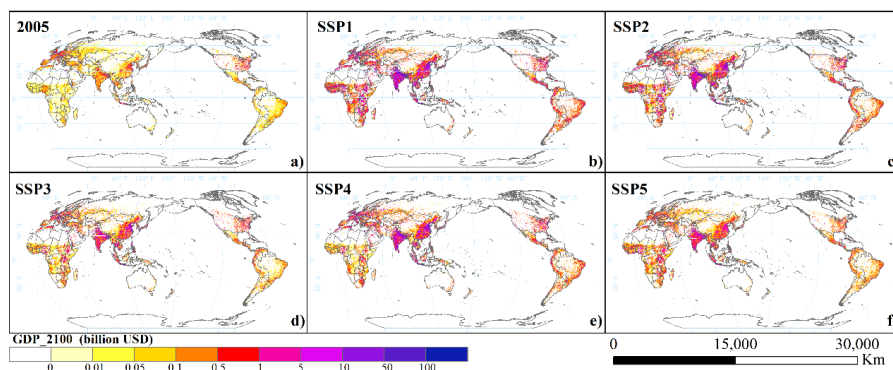




848  
849 Figure 3 The spatial allocation of global GDP using  $GDP_{Lit-Pop}$  approach for 2005 (a)  
850 and 2030 under SSP1-5 scenarios (b-f) at a spatial resolution of 1 km.  
851



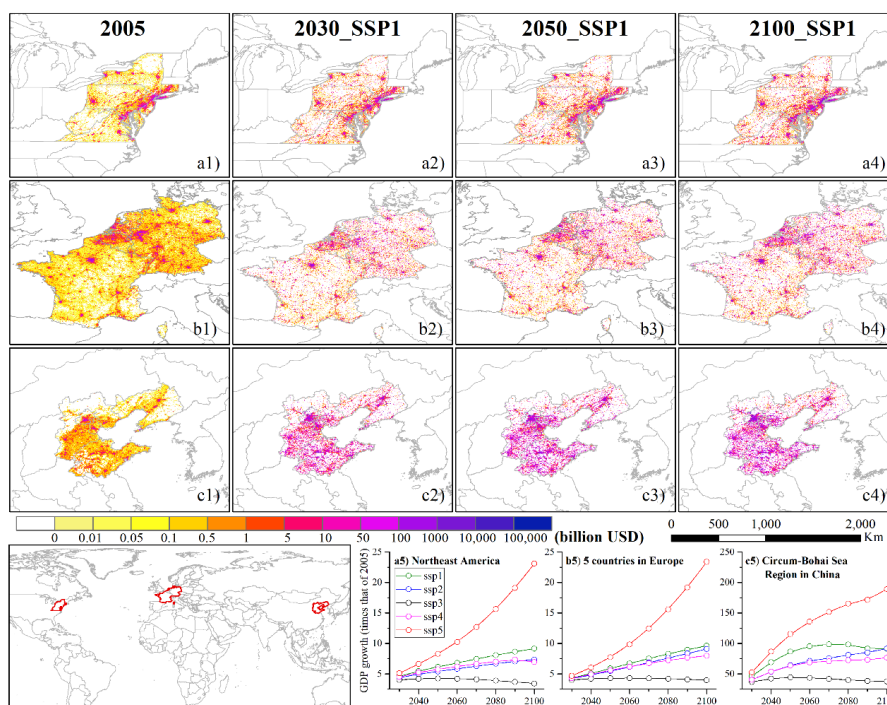
852  
853 Figure 4 The spatial allocation of global GDP using  $GDP_{Lit-Pop}$  approach for 2005 (a)  
854 and 2050 under SSP1-5 scenarios (b-f) at a spatial resolution of 1 km.  
855



856  
857 Figure 5 The spatial allocation of global GDP using  $GDP_{Lit-Pop}$  approach for 2005 (a)  
858 and 2100 under SSP1-5 scenarios (b-f) at a spatial resolution of 1 km.



859



860

861 Figure 6 The spatial allocation of GDP in selected regions (Northeast America (a series),  
862 five countries in Europe (b series), and Circum-Bohai Sea Region in China (c series))  
863 for 2005 as historical period and for 2030, 2050, and 2100 using  $GDP_{Lit-Pop}$  approach  
864 under SSP1 scenario as study case (1 km resolution). Their spatial distribution and  
865 corresponding regional GDP growth (times that of 2005) are in the bottom.

866

867

868

869